NONLINEAR BEHAVIOR OF STEEL PLATE BONDING CFRP SHEET UNDER UNIAXIAL TENSILE LOADING

Nagaoka University of Technology Regular Member ○ Ngoc Vinh PHAM
Nagaoka University of Technology Regular Member Takeshi MIYASHITA

1. INTRODUCTION

Carbon fiber-reinforced plastic (CFRP) in sheet form is usually applied to repair and strengthen steel structures which have reduced load-carrying capacity due to natural hazards, corrosion damages, and fatigue damage. To maximize the effectiveness of the repair and reinforcement method using CFRP sheets, and to prevent the peeling failure of CFRP layers under large deformations such as buckling (**Fig. 1**), the polyurea putty with a low elastic modulus (55 MPa-75 MPa) and high elongation (300%-500%) is usually inserted between the steel members and the CFRP sheet. Further, in many cases, peeling failure occurs in the CFRP sheet although the steel member is within the elastic range. Therefore, it is clear that the maximum strength of the steel members repaired or reinforced is often determined by the peeling failure of the interface between the structure and the CFRP sheet. For this reason, in order to perform the most effective repair and reinforcement, it is necessary to understand the mechanical behavior, peeling mechanism, and the peeling strength of the adhesion layer inserted between the steel member and the CFRP sheet. However, some studies proposed linear theoretical analysis to determine the peeling strength of the adhesion layer by calculating the principal stress on the adhesion layer, and there is no study in which nonlinear analysis has been mentioned. Therefore, this study established a nonlinear theoretical analysis method considering the nonlinear material condition of the steel plate, CFRP sheet, and adhesion layer; for steel plate bonding a layer of the CFRP sheet under uniaxial tensile loading. Moreover, in order to confirm the accuracy of the proposed theoretical analysis method, a two-dimensional geometric nonlinear finite element method (FEM) analysis was implemented.

Fig. 1 Peeling failure on steel members bonding CFRP sheets.

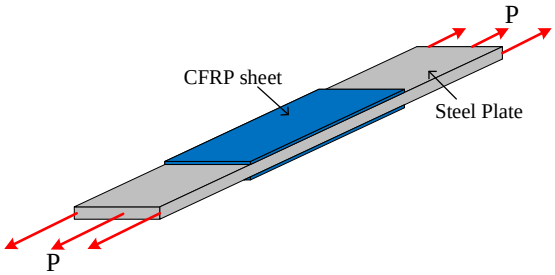

Fig. 2 Analytical object.

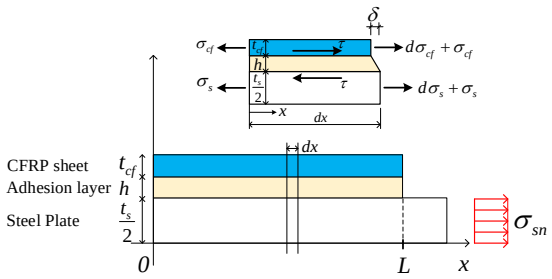

Fig. 3 Modeling (1/4 model).

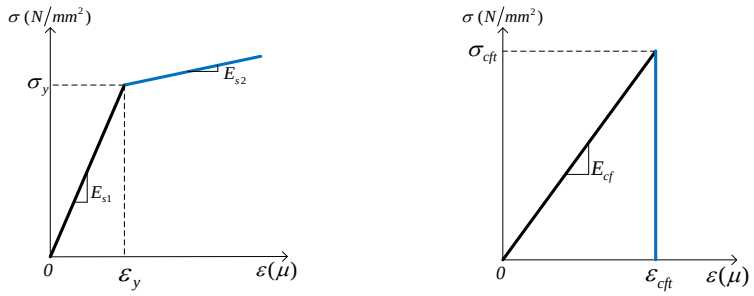

(a) Steel (σ-ε) (b) CFRP sheet (σ-ε) (c) Adhesion layer (τ-δ)

Fig. 4 Constitutive models of materials.

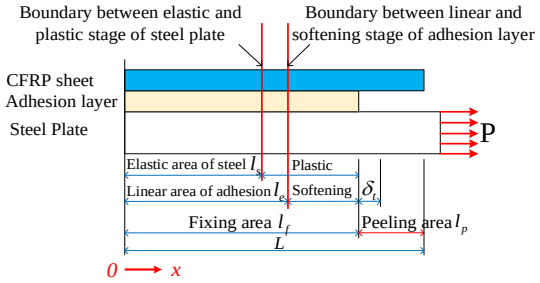

Fig. 5 Peeling mechanism of adhesion layer (1/4 model).

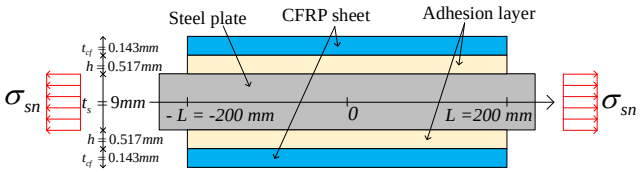

Fig. 6 Calculated model of the example.

Table 1 Material properties of steel, CFRP sheet, and adhesion layer.

Steel (SS400)		
E_{s1}	2 x 10^5	MPa
E_{s2}	2 x 10^3	MPa
σ_y	417	MPa
b	60	mm

CFRP sheet (FTS-C8-30)		
E_{cf}	6.4 x 10^5	MPa
σ_{cft}	2430	MPa
b	60	mm

Adhesion layer		
τ_y	17	MPa
δ_y	0.11	mm
δ_u	0.25	mm
b	60	mm

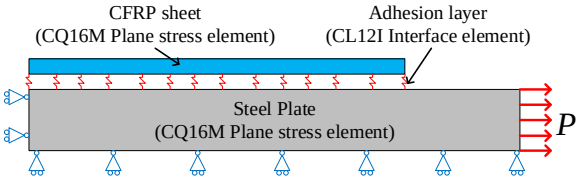

Fig. 7 Finite element analysis model.

2. THEORETICAL ANALYSIS

2.1 Analytical object

As the first premise of the nonlinear theoretical analysis method, this study used a steel plate bonding only one layer of CFRP sheet under uniaxial tensile loading (see **Fig. 2**), to determine the mechanical behavior, the peeling mechanism and the peeling strength of the adhesion layer inserted between the steel plate and CFRP sheet. In this analytical object, the width of CFRP sheet was the same with that of the steel plate. In addition, the principal direction of the CFRP sheet bonded was matched with that of the applied load.

2.2 Differential equation

The calculated model is described as a quarter model (**Fig. 3**) of the CFRP-sheet-bonded steel plate; and considered the nonlinear material condition of the steel plate, CFRP sheet, and the adhesion layer as shown in **Fig. 4**. Here, as a bonding constitution rule, it was generally assumed that the material model of the adhesion layer was considered by the relationship between shear stress and relative displacement, as shown in **Fig. 4**(c). Additionally, the elastic modulus of the adhesion layer was smaller by two orders of magnitude than that of steel and the CFRP sheet; hence, the adhesion layer was considered only shear stress, and the steel plate and the CFRP sheet was considered only tensile stress. The differential equations obtained from the balance equations of force and the material models is shown as follows.

In case of $0 \le \delta \le \delta_y$

$$\frac{d^2\delta(x)}{dx^2} - \left(\frac{2}{E_{s1}t_s} + \frac{1}{E_{cf}t_{cf}}\right)\frac{\tau_y}{\delta_y}\delta(x) = 0 \ \ if \ \left(\varepsilon_s \le \varepsilon_y\right) \tag{1a}$$

$$\frac{d^2\delta(x)}{dx^2} - \left(\frac{2}{E_{s2}t_s} + \frac{1}{E_{cf}t_{cf}}\right)\frac{\tau_y}{\delta_y}\delta(x) = 0 \ \ if \ \left(\varepsilon_s > \varepsilon_y\right) \tag{1b}$$

In case of $\delta_y < \delta \le \delta_u$

$$\frac{d^2\delta(x)}{dx^2} - \left(\frac{2}{E_{s1}t_s} + \frac{1}{E_{cf}t_{cf}}\right)\frac{\tau_y}{\delta_u - \delta_y}\left(\delta_u - \delta(x)\right) = 0 \ \ if \ \left(\varepsilon_s \le \varepsilon_y\right) \tag{2a}$$

$$\frac{d^2\delta(x)}{dx^2} - \left(\frac{2}{E_{s2}t_s} + \frac{1}{E_{cf}t_{cf}}\right)\frac{\tau_y}{\delta_u - \delta_y}\left(\delta_u - \delta(x)\right) = 0 \ \ if \ \left(\varepsilon_s > \varepsilon_y\right) \tag{2b}$$

2.3 Calculation process

The peeling mechanism of the adhesion layer on the analytical object of this study is shown in **Fig. 5**. In the analytical object, the peeling damage occurs when the maximum value of the relative displacement on the adhesion layer exceeds the value of δ_u of the adhesion material. Further, this maximum value was reached at the top of the fixing section of the bonded CFRP sheet. Therefore, to simplify the calculation process, the type of the applied load was the relative displacement. This means that the calculation process in the proposed theoretical analysis method was conducted by gradually increasing the relative displacement of δ_t at the top of the fixing section of CFRP sheet (see **Fig. 5)**.

Based on the level of the applied relative displacement and the material model of the adhesion layer, the calculation program was classified into the four stages; including the completely linear stage, softening stage, peeling stage, and the developing stage of peeling damage of adhesion layer. The stress and strain values on steel plate, CFRP layer, and adhesion layer were obtained by solving the general solutions of the differential conditions (1) and (2) at each of the applied load step. Unknown coefficients in the general solutions were determined from the continuous and boundary conditions for stress, strain and relative displacement in each member of the analytical model. Furthermore, l_s of the length of the elastic area on the steel plate, and l_e of the length of linear area on the adhesion layer were determined from the conditions of the convergence calculation, using the Newton-Raphson method. Additionally, at each step of the applied relative displacement load, the calculation program was stopped if the stress on CFRP layer was greater than the tensile strength of CFRP sheet.

3. EXAMPLE AND DISCUSSION

3.1 Calculation model

In the example, the calculated model and the material properties of all members are shown in **Fig. 6** and **Table 1**, respectively. The length and thickness of the steel plate were 400 mm and 9 mm, respectively; and 400 mm and 0.143 mm, respectively, regarding the CFRP sheet. In the

calculated model, the width of CFRP sheet was the same that of steel plate with 60 mm. the CFRP sheet was bonded to the steel plate by using an adhesion layer with the thickness of 0.517 mm. Moreover, carbon steel was used as a base metal. The stress-strain curve relationship of the carbon steel used in the calculated model was bilinear, in which the primary Young's modulus was $E_{s1} = 2x10^5$ MPa, and secondary modulus after yield was $E_{s2} = E_{s1}/100 =$ 2000 MPa. The Poisson ratio was 0.3, the yield stress was 417 MPa. The employed FTS-C8-30 CFRP, in sheet form, is lightweight (2.1 g/cm^3), has a large tensile strength (2430 MPa), and is durable in harsh environments. In particular, the FTS-C8-30 CFRP sheet has an elastic modulus that is 3.2 times higher than that of the steel with the elastic modulus of $6.4x10^5$ MPa. The constitutive model of the adhesion layer was used as the bilinear model proposed by Zhang et al.[1)]. This material model was formulated from the strain distribution measured on the 25 mm x 25 mm x 600 mm steel-plate-specimens bonding CFRP sheet under the uniaxial tensile tests. Its shear strength τ_y, relative displacement δ_y at shear strength, and relative displacement δ_u at the peeling stage are 17 MP, 0.11 mm, and 0.25 mm, respectively.

To confirm the accuracy of the proposed nonlinear theoretical method, a two-dimensional geometric nonlinear FEM analysis was implemented with a quarter model of the steel plate bonding a CFRP layer, using a distribution load as shown in **Fig. 7**. Further, the analysis software used in this study was DIANA 9.6. The steel plate and CFRP sheet were constructed of the plane stress element (the eight-node CQ16M). Moreover, the adhesion layer was simulated by using the interface element (the three-node CL12I element), which has the material models made up of the relationship between stress and relative displacement. The boundary conditions were considered on two symmetrical sides, with the fixed perpendicular direction, and free in the other direction (**Fig. 7)**.

3.2 Results of proposed method

The relationship between load and relative displacement at the top of the fixing location of the CFRP sheet is shown in **Fig. 8** to compare the FEM analytical (FEA) and the proposed theoretical analytical (CAL) results. The results of CAL indicate that the load-relative displacement curve began to change at the load of 225 kN (initial plastic load) because the stress on a part of the steel plate reached the plastic condition. Meanwhile at this load level, the CFRP sheet and the adhesion layer still worked at the linear stage. This trend was consistent with the behavior obtained in the result of FEA. Furthermore, the initial stiffness of the calculated model obtained from the FEA and CAL result was in complete agreement.

After overcoming the initial plastic load, the load-relative displacement curve was gradually bent until the peeling damage appears at the top of the fixing location of the CFRP sheet under a load of 247.52 kN. Then, the load value of the CFRP-sheet-bonded steel plate did not change significantly after the peeling damage occurred on the CFRP sheet. Further, the load value causing this peeling damage between the steel plate and the CFRP sheet was considered as the load-carrying capacity of the calculated model. All the trends described above were exactly the same as those obtained from the FEM analysis.

Figure 9 describes the stress distribution of the steel plate, CFRP sheet, and the adhesion layer obtained from the result of CAL and FEA at the loads of 100 kN, 239 kN, 245 kN, and 247.52 kN. The stress of the CFRP sheet was much smaller than its tensile strength during the loading process. **Fig. 9** also indicates the agreement between the CAL and FEA results. Under the load value of 100 kN, the mechanical behavior of all members of the calculated model was linear (**Fig. 9**(a)). At 239 kN, a part of the steel plate on the calculated model reached the plastic condition, and the stress of the adhesion layer at the top of the fixing section reached its shear strength (**Fig. 9**(b)). At 245 kN, a part of the adhesion layer reached the softening condition (**Fig. 9**(c)). Then, when the applied relative displacement value continued to increase to the value of $\delta_u = 0.25$ mm, the peeling damage of the adhesion layer began to appear at the load of 247.52 kN (**Fig. 9**(d)). This also means that the peeling strength of the adhesion layer was determined when the shear stress of the adhesion layer at the top of the fixing location of the CFRP sheet reached the value of zero (**Fig. 9**(d)). Therefore, the peeling strength of the example model was 247.52 kN.

4. CONCLUSION

For the steel members, which bonded a layer of the CFRP sheet under uniaxial-tensile-stress conditions; it was possible to clarify the actual peeling mechanism of the adhesion layer through the calculation procedure of the proposed nonlinear theoretical analysis method. Moreover, the comparison of the results with the FEM analytical results indicated that it was possible to accurately evaluate the peeling strength of the calculation model and the mechanical behavior of the steel plate, CFRP sheet, and the adhesion layer.

In future research, it will be necessary to develop the nonlinear theoretical analysis method for the model of the steel plate with multilayered CFRP sheet under uniaxial loading and bending; and the model which is able to fully consider the material properties (shear direction and normal direction) of the adhesion layer.

REFERENCE

1) Zhang, G., Hoshikuma, J., Sakai, J., and Unjoh, S.: Seismic Retrofit of RC Bridge Columns Using Combination of Carbon Fiber Reinforced Polymer Sheet and Steel Jacketting, *Journal of Japan Society of Civil Engineer (JSCE)*, Vol. 67, No. 2, pp. 430-445, 2011 (in Japanese).

2) Kamiharako, A., Shimomura, T., Maruyama, K., and Nishida, H.: Analysis of Bond and Debonding Behavior of Continuous Fiber Sheet Bonded on Concrete, *Journal of Japan Society of Civil Engineer (JSCE)*, No. 634/V-45, pp. 197-208, 1999.11 (in Japanese).

3) Miyashita, T., and Nagai, M.: Stress Analysis for Steel Plate with Multilayered CFRP under Uni-axial Loading, *Journal of Japan Society of Civil Engineer (JSCE)*, Vol. 66, No. 2, pp. 378-392, 2010.6 (in Japanese).

4) Okura, I., and Nagai, K.: Required Length and Debonding Shear Stress of Multiple CFRP Strips Bonded to steel Plate, *JSCE*, Vol. 67, No. 1, pp. 72-85, 2011.

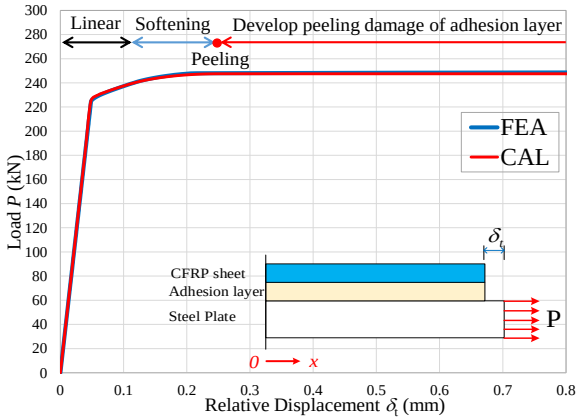

Fig. 8 Load-relative displacement relationship.

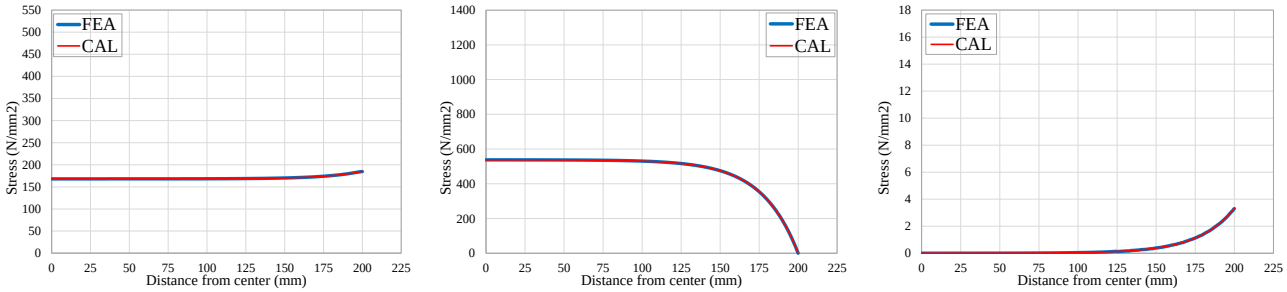

Steel plate CFRP sheet Adhesion layer

(a) At the load of 100 kN

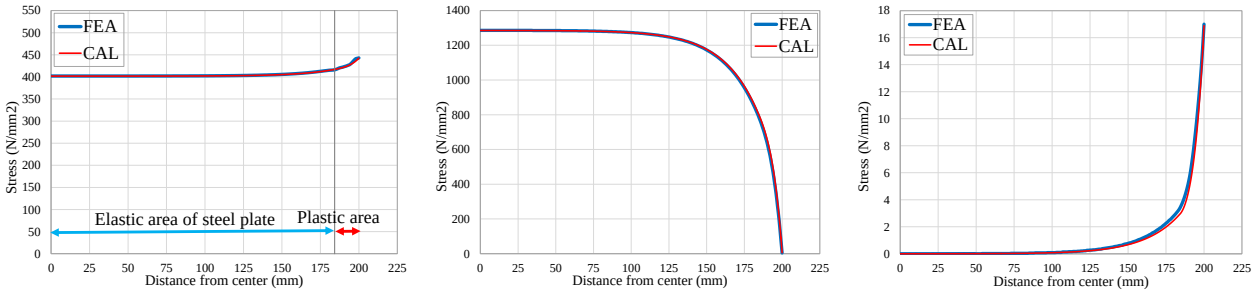

Steel plate CFRP sheet Adhesion layer

(b) At the load of 239 kN

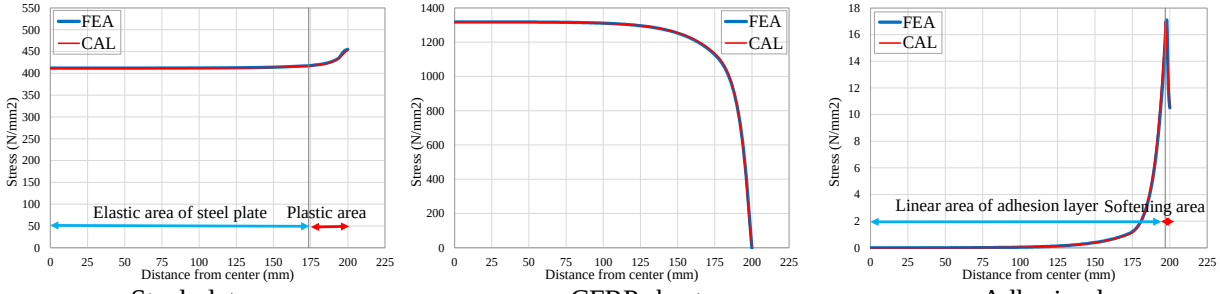

Steel plate CFRP sheet Adhesion layer

(c) At the load of 245 kN

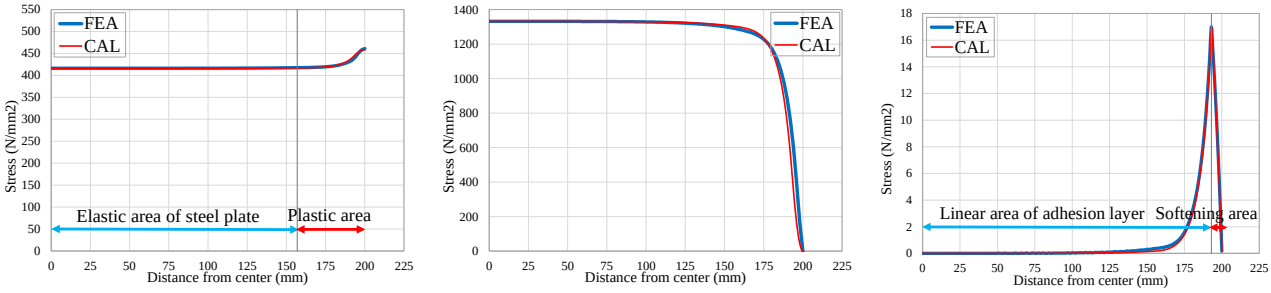

Steel plate CFRP sheet Adhesion layer

(d) At the load of 247.52 kN

Fig. 9 Comparison of stress distribution between CAL and FEA.